

Caspase-11 cleaves gasdermin D for non-canonical inflammasome signalling

Nobuhiko Kayagaki¹, Irma B. Stowe¹, Bettina L. Lee¹, Karen O'Rourke¹, Keith Anderson², Søren Warming², Trinna Cuellar², Benjamin Haley³, Merone Roose-Girma², Qui T. Phung³, Peter S. Liu³, Jennie R. Lill³, Hong Li³, Jiansheng Wu³, Sarah Kummerfeld⁴, Juan Zhang⁵, Wyne P. Lee⁵, Scott J. Snipas⁶, Guy S. Salvesen⁶, Lucy X. Morris⁷, Linda Fitzgerald⁷, Yafei Zhang⁷, Edward M. Bertram^{7,8}, Christopher C. Goodnow^{8,9,10} & Vishva M. Dixit¹

Intracellular lipopolysaccharide from Gram-negative bacteria including *Escherichia coli*, *Salmonella typhimurium*, *Shigella flexneri*, and *Burkholderia thailandensis* activates mouse caspase-11, causing pyroptotic cell death, interleukin-1 β processing, and lethal septic shock. How caspase-11 executes these downstream signalling events is largely unknown. Here we show that gasdermin D is essential for caspase-11-dependent pyroptosis and interleukin-1 β maturation. A forward genetic screen with ethyl-*N*-nitrosourea-mutagenized mice links *Gsdmd* to the intracellular lipopolysaccharide response. Macrophages from *Gsdmd*^{-/-} mice generated by gene targeting also exhibit defective pyroptosis and interleukin-1 β secretion induced by cytoplasmic lipopolysaccharide or Gram-negative bacteria. In addition, *Gsdmd*^{-/-} mice are protected from a lethal dose of lipopolysaccharide. Mechanistically, caspase-11 cleaves gasdermin D, and the resulting amino-terminal fragment promotes both pyroptosis and NLRP3-dependent activation of caspase-1 in a cell-intrinsic manner. Our data identify gasdermin D as a critical target of caspase-11 and a key mediator of the host response against Gram-negative bacteria.

Cytoplasmic caspase-11 (also known as caspase-4) defines the non-canonical inflammasome that is activated by various Gram-negative bacterial infections and causes infected cells to die by pyroptosis¹⁻⁴. Caspase-11 also triggers NLRP3- and ASC-dependent activation of caspase-1, resulting in the proteolytic maturation of the inactive cytokine pro-interleukin (IL)-1 β (refs 1, 5–7). Lipopolysaccharide (LPS) is the bacterial pathogen-associated molecular pattern that promotes caspase-11 activation^{7,8}. Cytoplasmic LPS can directly bind to and activate caspase-11 independently of Toll-like receptor 4 (TLR4)⁹, but precisely how caspase-11 executes pyroptosis and non-canonical NLRP3 inflammasome activation has remained unknown.

Phenomics identifies gasdermin D

An unbiased forward genetic screen with ethyl-*N*-nitrosourea (ENU)-mutagenized mice¹⁰ was performed to unveil essential mediators of non-canonical inflammasome signalling in response to cytoplasmic LPS. Pedigree IGL1351 had a Mendelian recessive mutation that compromised LPS-induced IL-1 β secretion from peritoneal macrophages. The severity of the defect was equivalent to that seen with the *Casp11* mutant 129 strain¹ (Fig. 1a and Extended Data Fig. 1). Importantly, IL-1 β secretion by pedigree IGL1351 in response to *Clostridium difficile* toxin B (TcdB), a stimulant of the Mediterranean fever/Pyrim canonical inflammasome^{11,11}, was comparable to other pedigrees. Exome sequencing identified 39 single-nucleotide variants (SNVs) in the ENU-mutated founder G1 male. Subsequent genotyping of all identified SNVs in a large cohort of siblings and offspring revealed that the trait was completely correlated with inheritance of a point mutation in the gene encoding gasdermin D (*Gsdmd*) (Extended Data Fig. 1 and Extended Data Table 1).

Gsdmd (ref. 12) is a 487 amino acid cytoplasmic protein that contains an ill-characterized gasdermin domain and lacks any obvious signal

peptide or transmembrane segments (Fig. 1b). The human gasdermin gene family consists of *GSDMA*, *GSDMB*, *GSDMC* and *GSDMD*. The physiological role of *Gsdmd* is unknown¹³, although other gasdermin family members have been implicated in deafness or apoptosis in epithelial cells^{12,14}. The ENU-derived mutation in *Gsdmd* caused an Ile to Asn amino acid substitution at position 105 with a PolyPhen score of 0.98 (probably damaging) and a SIFT (sorting intolerant from tolerant) score of 0.00 (deleterious) (Fig. 1b and Extended Data Table 1). Full-length *Gsdmd* protein (53 kDa) was immunoblotted in unstimulated wild-type bone-marrow-derived macrophages (BMDMs). Unlike pro-caspase-11, *Gsdmd* was not induced to any great extent by TLR agonists or interferons (Fig. 1c). Wild-type and *Gsdmd*^{I105N/I105N} BMDMs expressed comparable amounts of *Gsdmd* (Fig. 1d), suggesting that the I105N mutation impairs *Gsdmd* function rather than protein expression.

Wild-type, *Casp11*^{-/-}, or *Gsdmd*^{I105N/I105N} BMDMs that were primed with Pam3CSK4 and then stimulated with canonical inflammasome stimuli, including ATP to engage the NLRP3-dependent inflammasome⁶, poly(dA:dT) double-stranded DNA (dsDNA) to activate the AIM2-dependent inflammasome^{15–17}, or TcdB¹¹, secreted comparable amounts of IL-1 β and exhibited similar levels of pyroptotic death¹ (Fig. 1e). Consistent with these data, *Gsdmd*^{I105N/I105N} BMDMs displayed normal induction of NLRP3, pro-IL-1 β , and RANTES cytokine in response to TLR agonists (Fig. 1d, Extended Data Fig. 2a). *Gsdmd*^{I105N/I105N} BMDMs also upregulated pro-caspase-11 normally (Fig. 1d) but, in contrast to their wild-type counterparts, were defective in IL-1 β secretion, and did not undergo pyroptosis in response to cytoplasmic LPS (Fig. 1e). Proteolytic processing of caspase-1 and pro-IL-1 β preceding IL-1 β secretion was also impaired, suggesting that *Gsdmd* is critical for all caspase-11-dependent signalling events (Extended Data Fig. 2b).

¹Department of Physiological Chemistry, Genentech Inc., South San Francisco, California 94080, USA. ²Department of Molecular Biology, Genentech Inc., South San Francisco, California 94080, USA.

³Department of Protein Chemistry, Genentech Inc., South San Francisco, California 94080, USA. ⁴Department of Bioinformatics, Genentech Inc., South San Francisco, California 94080, USA. ⁵Department of Immunology, Genentech Inc., South San Francisco, California 94080, USA. ⁶Program in Cell Death Signaling Networks, Sanford-Burnham-Prebys Medical Discovery Institute, La Jolla, California 92037, USA. ⁷The Australian Phenomics Facility, The John Curtin School of Medical Research, The Australian National University, Canberra, Australian Capital Territory 2601, Australia. ⁸Department of Immunology and Infectious Diseases, The John Curtin School of Medical Research, The Australian National University, Canberra, Australian Capital Territory 2601, Australia. ⁹Garvan Institute of Medical Research, Sydney, New South Wales 2010, Australia. ¹⁰St. Vincent's Clinical School, UNSW Australia, Darlinghurst, New South Wales 2010, Australia.

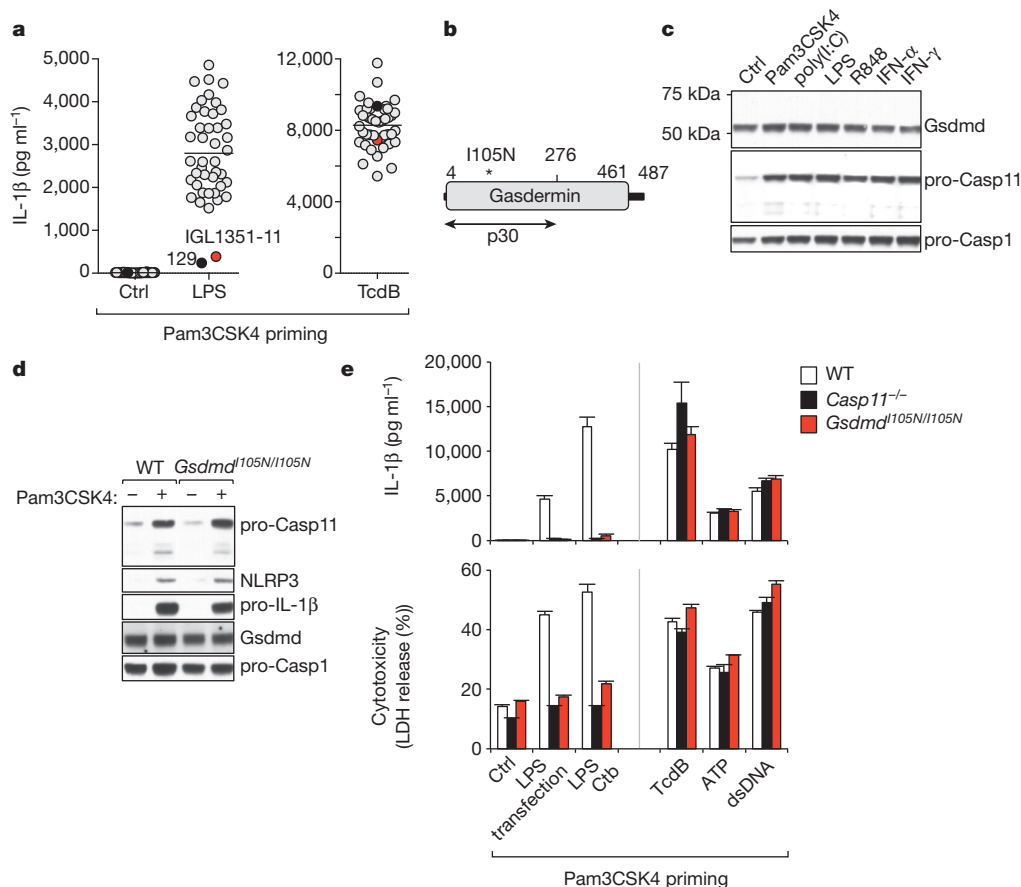


Figure 1 | *Gsdmd* mutation I105N abolishes non-canonical inflammasome signalling. **a**, Screening of third-generation offspring from ENU-treated C57BL/6 mice. Graphs indicate IL-1 β released from peritoneal macrophages cultured for 16 h. Circles indicate *Casp11* mutant 129 (black), IGL1351-11 (red), and other G3 offspring (grey). Centre bars represent averages. **b**, Schematic of mouse Gsdmd. Gasdermin domain is grey (Pfam PF04598).

Gsdmd is essential for caspase-11 signalling

We confirmed a critical role for Gsdmd in non-canonical inflammasome signalling using gene-targeted *Gsdmd*^{-/-} mice. In control experiments, Pam3CSK4-primed wild-type, *Gsdmd*^{-/-}, and *Casp11*^{-/-} BMDMs exhibited equivalent caspase-1-dependent IL-1 β secretion and pyroptosis after a 16 h treatment with TcdB, ATP, dsDNA, or the NLR4 inflammasome trigger flagellin¹⁸ (Fig. 2a and Extended Data Fig. 3a, b). The effect of Gsdmd deficiency on caspase-1-dependent pyroptosis at earlier time points is discussed in a later section. Caspase-11 or Gsdmd deficiency also had no effect on IL-1 β secretion in response to other canonical NLRP3 inflammasome stimuli including listeriolysin O (LLO) toxin, monosodium urate (MSU), lysomotropic agent HLLoMe, or calcium pyrophosphate (CPPD)^{1,19–22} (Extended Data Fig. 3c, d). In keeping with these data, TLR agonists induced NLRP3, pro-caspase-11, and RANTES to a similar extent in wild-type and *Gsdmd*^{-/-} BMDMs (Extended Data Fig. 3a, e). Therefore, Gsdmd is dispensable for normal TLR priming. *Gsdmd*^{-/-} BMDMs were, however, resistant to pyroptosis and failed to secrete IL-1 β when transfected with *E. coli* LPS or synthetic monophosphoryl lipid A, the active moiety of LPS^{7,8} (Fig. 2a, Extended Data Fig. 3b). *Gsdmd*^{-/-} BMDMs were also unresponsive to electroporated LPS, or LPS transfected with cholera toxin B complex⁷, or *S. typhimurium* LPS (Extended Data Fig. 3f). *Gsdmd*, like *Casp11*, was also required for processing of pro-caspase-1 and pro-IL-1 β in response to cytoplasmic LPS (Fig. 2b). Finally, *Gsdmd*^{-/-} BMDMs further resembled *Casp11*^{-/-} BMDMs in failing to secrete IL-1 β or undergo pyroptosis upon infection with Gram-negative bacteria (*E. coli*, *Citrobacter rodentium*, or *Shigella flexneri*), whereas both genotypes

c, d, Immunoblots of wild-type (WT) BMDMs (**c**) or the genotypes indicated (**d**) after 6 h culture. **e**, IL-1 β and LDH released from BMDMs after 16 h. Graphs show mean \pm s.d. of triplicate wells and represent three independent experiments. LPS Ctb, LPS plus cholera toxin B complex. For source gels of **c** and **d**, see Supplementary Fig. 1.

responded normally to *Pseudomonas aeruginosa* that activates the NLR4 canonical inflammasome^{1,3,7,23} (Fig. 2c). Collectively, these data confirm that macrophages require Gsdmd for pyroptosis and IL-1 β secretion in response to intracellular LPS.

Human caspase-4 and caspase-5, the orthologues of mouse caspase-11, induce pyroptosis in myeloid and endothelial cells in response to intracellular LPS^{9,24}. Like caspase-4/5/11, *Gsdmd* is specific to mammals^{14,25}, suggesting a co-emergence of those genes. Human GSDMD exhibits 58% amino acid sequence identity with mouse Gsdmd. Deletion of *GSDMD* or *CASP4* by CRISPR/Cas9 in human EA.hy926 endothelial cells or human THP-1 monocytes did not affect death induced by APO2L²⁶ or dsDNA, but it completely abolished intracellular LPS-induced cytotoxicity (Fig. 2d, Extended Data Fig. 3g–i). Thus, human GSDMD is required for the caspase-4-dependent response to cytoplasmic LPS.

Caspase-11 cleaves and activates Gsdmd

We next questioned how Gsdmd promotes pyroptosis and caspase-1 activation by the non-canonical inflammasome. We noticed that BMDMs transfected with LPS exhibited caspase-11-dependent cleavage of Gsdmd, giving rise to a 30-kDa N-terminal Gsdmd fragment (Fig. 3a). These data identified Gsdmd as a potential substrate of caspase-11. Recombinant caspase-11 cleaves artificial peptide substrates after an aspartate residue^{27,28}, but physiological substrates of caspase-11 are not well defined. Purified recombinant Gsdmd was cleaved by recombinant caspase-11 *in vitro* into two fragments. Edman sequencing mapped the cleavage site in Gsdmd to LLSD₂₇₆↓G₂₇₇ (Fig. 3b). The

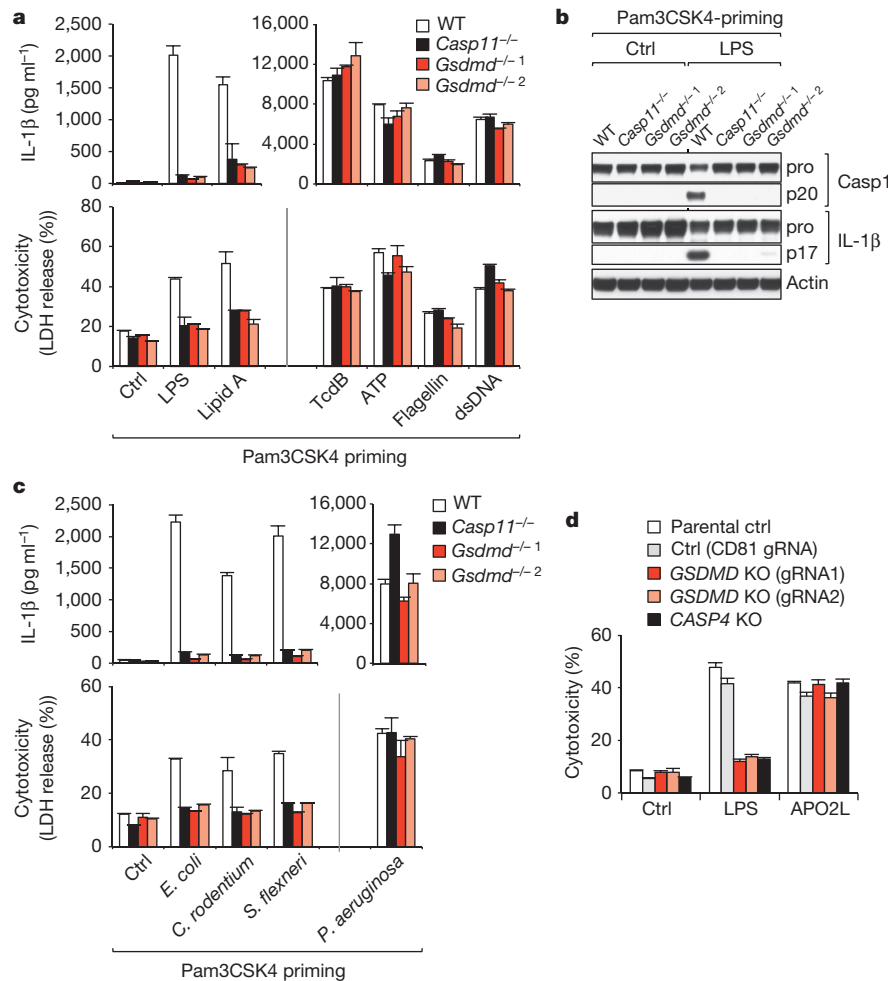


Figure 2 | Gsdmd is essential for non-canonical inflammasome signalling.

a, c, IL-1 β and LDH released from BMDMs after 16 h. *P. aeruginosa* infection was analysed after 4 h. *Gsdmd*^{-/-1} and *Gsdmd*^{-/-2} are independent knockout strains. **b**, Immunoblots of pooled cell extracts and supernatants from BMDMs at 6 h after electroporation with LPS. For source gels, see Supplementary Fig. 1.

d, Cytotoxicity of APO2L or transfected LPS on control, *GSDMD*-knockout, or *CASP4*-knockout EA.hy926 cells after 16 h. Graphs show mean \pm s.d. of triplicate wells and represent three independent experiments. gRNA, single-guide RNA.

P₁-Asp cleavage residue and P₁'-Gly residues are conserved across species (Extended Data Fig. 4a). Ectopic expression of the N-terminal Gsdmd cleavage fragment (mouse residues 1–276) killed HEK293T cells, whereas expression of full-length Gsdmd or the C-terminal cleavage fragment did not (Fig. 3c). Collectively, these data indicate that caspase-11 directly cleaves the 53-kDa inactive precursor form of Gsdmd (pro-Gsdmd) to generate the pro-pyptotic N-terminal fragment (Gsdmd p30, Fig. 1b). In full-length Gsdmd, the C terminus may mask key sites in the N terminus until cleavage at D₂₇₆/G₂₇₇ releases this inhibition. Consistent with this notion, reconstitution of immortalized *Gsdmd*^{-/-} macrophages with wild-type Gsdmd restored LPS responsiveness, as evidenced by lactate dehydrogenase (LDH) release, IL-1 β secretion and caspase-1 processing, whereas reconstitution with the Gsdmd processing mutant D276A did not (Fig. 3d, e). In addition, mutation of Gsdmd within the p30 fragment (I105N) attenuated pyroptosis and caspase-1/IL-1 β processing (Fig. 1b, e and Extended Data Fig. 2b) without affecting Gsdmd cleavage (Extended Data Fig. 4b). These data confirm that conversion of pro-Gsdmd to its mature p30 form by caspase-11 is essential for both pyroptosis and caspase-1 activation in response to cytoplasmic LPS.

Cytoplasmic LPS also caused caspase-4-dependent processing of GSDMD in human THP-1 monocytes (Extended Data Fig. 5a). Furthermore, transient overexpression of caspase-4 or caspase-5 caused

human GSDMD cleavage to the pro-pyptotic p30 fragment (Extended Data Fig. 5b and c). These data together with the conserved P₁ and P₁' residues in GSDMD (Extended Data Fig. 4a) indicate a conserved mechanism of GSDMD activation by caspase-4/5/11.

Cytoplasmic LPS induces caspase-11-dependent pyroptosis and secretion of IL-1 β , but only the latter requires caspase-1, NLRP3 and ASC^{1,7}. Loss of NLRP3, ASC, or caspase-1 in BMDMs did not markedly affect caspase-11-dependent generation of mature Gsdmd p30 in response to cytoplasmic LPS (Fig. 4a), indicating that Gsdmd cleavage occurs upstream of NLRP3 inflammasome activation. The question arises as to whether Gsdmd induces pyroptosis and NLRP3 inflammasome activation simultaneously in the same cell, or if Gsdmd-mediated pyroptosis releases damage-associated molecular patterns²⁹ that trigger caspase-11-independent NLRP3 inflammasome activation in neighbouring cells (Extended Data Fig. 6a). We believe the latter hypothesis is unlikely because LPS-stimulated *Il1b*^{-/-} BMDMs exhibited normal pyroptosis, yet their culture supernatant failed to induce IL-1 β secretion from *Casp11*^{-/-} BMDMs (Extended Data Fig. 6b, c). In addition, *Casp11*^{-/-} BMDMs co-cultured with *Il1b*^{-/-} BMDMs did not secrete IL-1 β in response to cytoplasmic LPS (Fig. 4b and Extended Data Fig. 6d), making it unlikely that a paracrine signalling mechanism activates the NLRP3 inflammasome³⁰. Collectively, our data demonstrate that Gsdmd maturation by caspase-11 triggers two distinct cell-intrinsic signals:

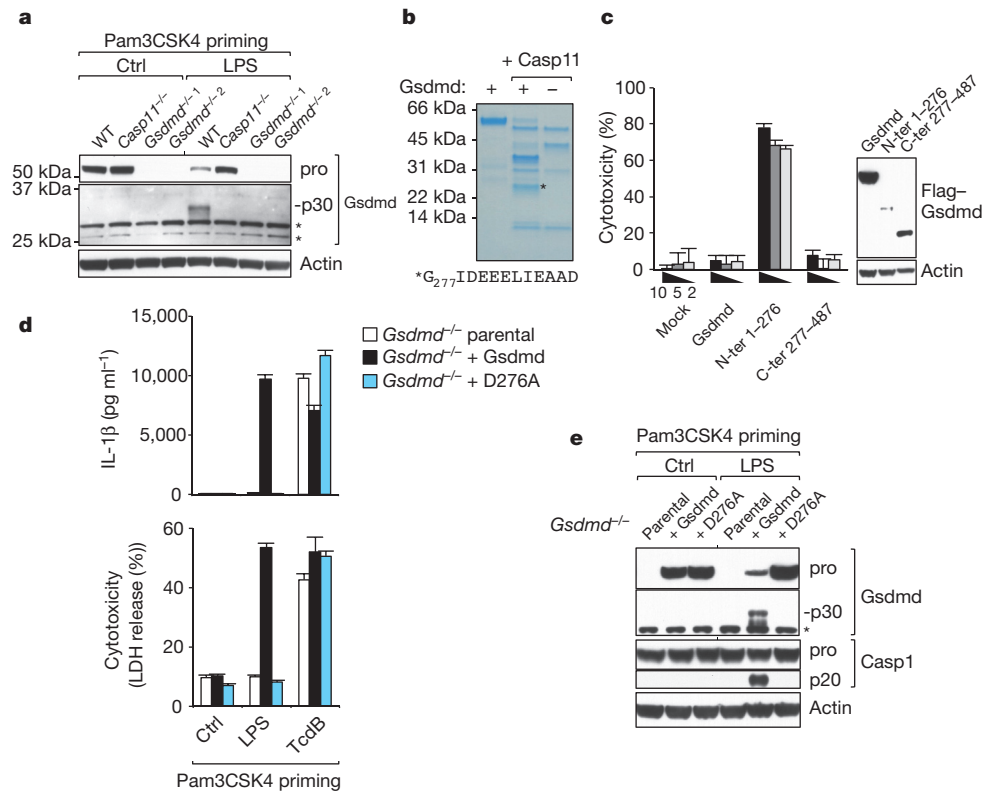


Figure 3 | Caspase-11 cleaves Gsdmd. **a**, Immunoblots of BMDM extracts and supernatants at 6 h after LPS electroporation. Non-specific bands are indicated with asterisks. **b**, Coomassie blue staining of Gsdmd incubated with caspase-11. N terminus of the band marked with an asterisk is shown. **c**, Cytotoxicity of mouse Gsdmd in HEK293Ts. Numbers indicate nanograms of plasmid transfected. **d**, IL-1β and LDH released from reconstituted

Gsdmd^{-/-} immortalized macrophages at 16 h after LPS transfection. **e**, Immunoblots of immortalized macrophage extracts and supernatants in **d**. Non-specific band is indicated with an asterisk. Graphs show mean ± s.d. of triplicate wells and represent three independent experiments. For source gels of **a**, **c**, and **e**, see Supplementary Fig. 1.

(i) pyroptosis induction; and (ii) NLRP3-dependent caspase-1 activation (Fig. 4c).

Role for Gsdmd in canonical pyroptosis

Human caspase-1 is reported to cleave GSDMD at the same P₁-Asp residue³¹ as caspase-11, albeit that the preferred tetrapeptide cleavage sequence of caspase-1 differs from that of caspase-11^{27,28}. Consistent with this study³¹, the Gsdmd p30 fragment appeared in BMDMs treated with canonical inflammasome activators including ATP (Fig. 5a and Extended Data Fig. 7a). Although *Gsdmd*^{-/-} BMDMs stimulated with ATP or flagellin underwent pyroptosis normally after 8 h, they exhibited less pyroptosis than wild-type BMDMs at earlier

time points (Figs 2a and 5c and Extended Data Fig. 7b). These data suggest that Gsdmd is also a physiological substrate of caspase-1. However, given that caspase-1-dependent pyroptosis is delayed rather than prevented, we believe that other ill-defined caspase-1 substrates can also mediate pyroptosis (Fig. 5d). This notion is in keeping with the fact that caspase-1 orthologues are found in vertebrates including non-mammals, whereas caspase-4/5/11 and *Gsdmd* are exclusive to mammals^{14,25,32}. Consistent with IL-1β being a direct substrate of caspase-1³³, *Gsdmd* deficiency did not impact caspase-1-dependent IL-1β processing in response to ATP (Fig. 5b). However, *Gsdmd*^{-/-} BMDMs secreted less IL-1β than wild-type at the 2-h time points in response to ATP and flagellin (Extended Data Fig. 7c). Gsdmd may

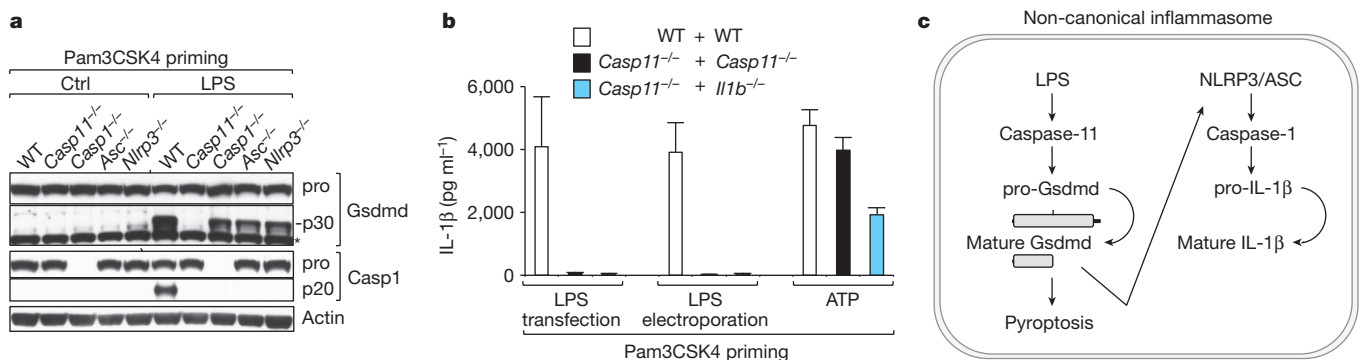


Figure 4 | Cell-intrinsic NLRP3 inflammasome activation. **a**, Immunoblots of BMDM extracts and supernatants at 6 h after electroporation with LPS. Non-specific band is indicated with an asterisk. For source gels, see Supplementary Fig. 1. **b**, IL-1β released from 1:1 mixed BMDM cultures at 16 h after

stimulation. **c**, Model for non-canonical inflammasome signalling. Graph shows mean ± s.d. of triplicate wells and represents three independent experiments.

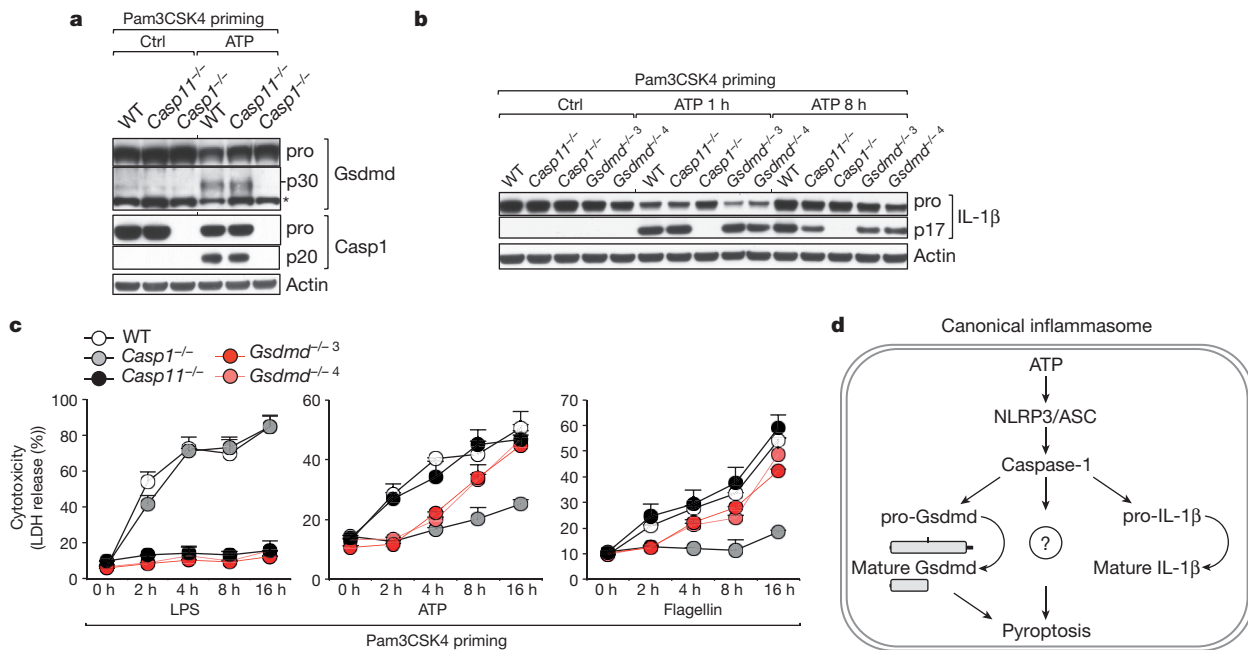


Figure 5 | Role of Gsdmd in canonical inflammasome signalling. **a, b**, Immunoblots of BMDM extracts and supernatants after stimulation with ATP for 8 h (**a**) or as indicated (**b**). Non-specific band is indicated with an asterisk. For source gels, see Supplementary Fig. 2. **c**, LDH released from

BMDMs after LPS electroporation or the treatments indicated. *Gsdmd*^{-/-} and *Gsdmd*^{-/-} are independent knockout strains. **d**, Model for canonical inflammasome signalling. Graphs show mean \pm s.d. of triplicate wells and represent three independent experiments.

contribute to IL-1 β release by damaging cell membranes or regulating the ill-characterized IL-1 β secretion mechanism^{34,35}.

Gsdmd is essential for lethal sepsis

We investigated the relevance of our *in vitro* findings in a mouse model of acute septic shock wherein caspase-11-dependent pyroptosis leads to lethal endotoxemia^{1,36}. Mice lacking either *Casp11* or *Gsdmd* were resistant to LPS-induced lethal septic shock (Fig. 6 and Extended Data Table 2). This result is consistent with Gsdmd being a critical pro-pyrototic substrate of caspase-11 *in vivo*.

Discussion

Pyroptosis plays an important role in anti-bacterial innate immune defence and lethal endotoxemia^{1,37,38}, but how inflammatory caspases 1, 4, 5 and 11 cause pyroptosis has remained unknown. Our data reveal that proteolytic cleavage of Gsdmd by mouse caspase-11 or human caspase-4 is essential for pyroptosis of innate immune cells and endothelial cells harbouring LPS-tainted cytoplasm. Cleaved Gsdmd also triggers NLRP3-dependent activation of caspase-1 through a cell-intrinsic pathway (Fig. 4c), although the exact mechanism responsible for NLRP3

activation remains unclear. NLRP3 senses diverse stimuli that perturb intracellular homeostasis^{6,19,21,22}, so its activation may be an indirect consequence of the effects of the Gsdmd p30 fragment. Future studies will need to address exactly what the p30 fragment does in cells. The re-defined non-canonical inflammasome signalling pathway (Fig. 4c) refutes the previous hypothesis that a caspase-1/11 complex is responsible for caspase-1 activation^{1,36}.

The partial contribution of Gsdmd to caspase-1-dependent pyroptosis suggests the existence of other pro-pyrototic caspase-1 substrates (Fig. 5d). Caspase-1 can trigger pyroptosis in the absence of Gsdmd, which is not unexpected because non-mammalian vertebrates lack *Gsdmd* yet still exhibit caspase-1-dependent pyroptosis^{14,25,32,39}. The co-emergence of caspase-4/5/11 and *Gsdmd* genes in the early stages of mammalian evolution might indicate co-evolution, perhaps in response to the need for additional anti-pathogen responses against Gram-negative bacteria.

Like other caspases, caspase-11 cleaves multiple substrates^{28,31,40}. However, our *in vitro* and *in vivo* data show that caspase-11 relies exclusively on Gsdmd to promote pyroptosis, caspase-1 activation and LPS-induced lethal sepsis. Thus Gsdmd is revealed as an unexpected, but critical facet of the anti-bacterial response.

Online Content Methods, along with any additional Extended Data display items and Source Data, are available in the online version of the paper; references unique to these sections appear only in the online paper.

Received 14 July; accepted 4 September 2015.

Published online 16 September 2015.

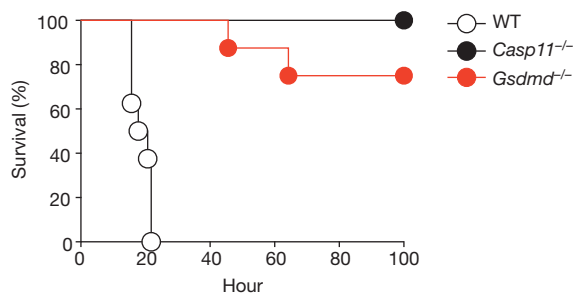


Figure 6 | Gsdmd deficiency protects against lethal sepsis. Kaplan-Meier survival plots for mice ($n = 8$ for each genotype) challenged with 54 mg kg⁻¹ LPS. *Gsdmd*^{-/-} mice were used (described in Extended Data Fig. 8). Statistical analysis and *P* values (Extended Data Table 2) were adjusted to account for multiple comparisons using Bonferroni's correction.

- Kayagaki, N. *et al.* Non-canonical inflammasome activation targets caspase-11. *Nature* **479**, 117–121 (2011).
- Broz, P. *et al.* Caspase-11 increases susceptibility to *Salmonella* infection in the absence of caspase-1. *Nature* **490**, 288–291 (2012).
- Rathinam, V. A. *et al.* TRIF licenses caspase-11-dependent NLRP3 inflammasome activation by gram-negative bacteria. *Cell* **150**, 606–619 (2012).
- Aachoui, Y. *et al.* Caspase-11 protects against bacteria that escape the vacuole. *Science* **339**, 975–978 (2013).
- Mariathasan, S. *et al.* Differential activation of the inflammasome by caspase-1 adaptors ASC and Ipaf. *Nature* **430**, 213–218 (2004).
- Mariathasan, S. *et al.* Cryopyrin activates the inflammasome in response to toxins and ATP. *Nature* **440**, 228–232 (2006).

7. Kayagaki, N. *et al.* Noncanonical inflammasome activation by intracellular LPS independent of TLR4. *Science* **341**, 1246–1249 (2013).
8. Hagar, J. A., Powell, D. A., Achoui, Y., Ernst, R. K. & Miao, E. A. Cytoplasmic LPS activates caspase-11: implications in TLR4-independent endotoxic shock. *Science* **341**, 1250–1253 (2013).
9. Shi, J. *et al.* Inflammatory caspases are innate immune receptors for intracellular LPS. *Nature* **514**, 187–192 (2014).
10. Nelms, K. A. & Goodnow, C. C. Genome-wide ENU mutagenesis to reveal immune regulators. *Immunity* **15**, 409–418 (2001).
11. Xu, H. *et al.* Innate immune sensing of bacterial modifications of Rho GTPases by the PIRIN inflammasome. *Nature* **513**, 237–241 (2014).
12. Katoh, M. & Katoh, M. Identification and characterization of human DFNA5L, mouse Dfna5l, and rat Dfna5l genes *in silico*. *Int. J. Oncol.* **25**, 765–770 (2004).
13. Fujii, T. *et al.* Gasdermin D (Gsdmd) is dispensable for mouse intestinal epithelium development. *Genesis* **46**, 418–423 (2008).
14. Tamura, M. *et al.* Members of a novel gene family, *Gsdm*, are expressed exclusively in the epithelium of the skin and gastrointestinal tract in a highly tissue-specific manner. *Genomics* **89**, 618–629 (2007).
15. Roberts, T. L. *et al.* HIN-200 proteins regulate caspase activation in response to foreign cytoplasmic DNA. *Science* **323**, 1057–1060 (2009).
16. Fernandes-Alnemri, T. *et al.* The AIM2 inflammasome is critical for innate immunity to *Francisella tularensis*. *Nature Immunol.* **11**, 385–393 (2010).
17. Hornung, V. *et al.* AIM2 recognizes cytosolic dsDNA and forms a caspase-1-activating inflammasome with ASC. *Nature* **458**, 514–518 (2009).
18. Franchi, L. *et al.* Cytosolic flagellin requires Ipaf for activation of caspase-1 and interleukin 1 β in salmonella-infected macrophages. *Nature Immunol.* **7**, 576–582 (2006).
19. Meixenberger, K. *et al.* *Listeria monocytogenes*-infected human peripheral blood mononuclear cells produce IL-1 β , depending on listeriolysin O and NLRP3. *J. Immunol.* **184**, 922–930 (2010).
20. Schroder, K. & Tschopp, J. The inflammasomes. *Cell* **140**, 821–832 (2010).
21. Martinon, F., Petrilli, V., Mayor, A., Tardivel, A. & Tschopp, J. Gout-associated uric acid crystals activate the NALP3 inflammasome. *Nature* **440**, 237–241 (2006).
22. Hornung, V. *et al.* Silica crystals and aluminum salts activate the NALP3 inflammasome through phagosomal destabilization. *Nature Immunol.* **9**, 847–856 (2008).
23. Sutterwala, F. S. *et al.* Immune recognition of *Pseudomonas aeruginosa* mediated by the IPAF/NLRC4 inflammasome. *J. Exp. Med.* **204**, 3235–3245 (2007).
24. Casson, C. N. *et al.* Human caspase-4 mediates noncanonical inflammasome activation against gram-negative bacterial pathogens. *Proc. Natl Acad. Sci. USA* **112**, 6688–6693 (2015).
25. Sakamaki, K. & Satou, Y. Caspases: evolutionary aspects of their functions in vertebrates. *J. Fish Biol.* **74**, 727–753 (2009).
26. Ashkenazi, A. & Dixit, V. M. Death receptors: signaling and modulation. *Science* **281**, 1305–1308 (1998).
27. Thornberry, N. A. *et al.* A combinatorial approach defines specificities of members of the caspase family and granzyme B. Functional relationships established for key mediators of apoptosis. *J. Biol. Chem.* **272**, 17907–17911 (1997).
28. Kang, S. J. *et al.* Dual role of caspase-11 in mediating activation of caspase-1 and caspase-3 under pathological conditions. *J. Cell Biol.* **149**, 613–622 (2000).
29. Kaczmarek, A., Vandenabeele, P. & Krysko, D. V. Necroptosis: the release of damage-associated molecular patterns and its physiological relevance. *Immunity* **38**, 209–223 (2013).
30. Rühl, S. & Broz, P. Caspase-11 activates a canonical NLRP3 inflammasome by promoting K⁺ efflux. *Eur. J. Immunol.* <http://dx.doi.org/10.1002/eji.201545772> (2015).
31. Agard, N. J., Maltby, D. & Wells, J. A. Inflammatory stimuli regulate caspase substrate profiles. *Mol. Cell. Proteomics* **9**, 880–893 (2010).
32. Angosto, D. *et al.* Evolution of inflammasome functions in vertebrates: Inflammasome and caspase-1 trigger fish macrophage cell death but are dispensable for the processing of IL-1 β . *Innate Immun.* **18**, 815–824 (2012).
33. Thornberry, N. A. *et al.* A novel heterodimeric cysteine protease is required for interleukin-1 beta processing in monocytes. *Nature* **356**, 768–774 (1992).
34. Eder, C. Mechanisms of interleukin-1 β release. *Immunobiology* **214**, 543–553 (2009).
35. Liu, T. *et al.* Single-cell imaging of caspase-1 dynamics reveals an all-or-none inflammasome signaling response. *Cell Rep.* **8**, 974–982 (2014).
36. Wang, S. *et al.* Murine caspase-11, an ICE-interacting protease, is essential for the activation of ICE. *Cell* **92**, 501–509 (1998).
37. Miao, E. A. *et al.* Caspase-1-induced pyroptosis is an innate immune effector mechanism against intracellular bacteria. *Nature Immunol.* **11**, 1136–1142 (2010).
38. Bergsbaken, T., Fink, S. L. & Cookson, B. T. Pyroptosis: host cell death and inflammation. *Nature Rev. Microbiol.* **7**, 99–109 (2009).
39. Xie, H. X. *et al.* *Edwardsiella tarda*-induced cytotoxicity depends on its type III secretion system and flagellin. *Infect. Immun.* **82**, 3436–3445 (2014).
40. Py, B. F. *et al.* Caspase-11 controls interleukin-1 β release through degradation of TRPC1. *Cell Rep.* **6**, 1122–1128 (2014).

Supplementary Information is available in the online version of the paper.

Acknowledgements We thank the staff of the Australian Phenomics Facility, Genentech Transgenic Technology and FACS cores, and K. Bowman, J. Payandeh, E. Dueber, R. Aglietti, A. Gupta and A. Peterson for technical expertise and discussion, K. Newton for manuscript editing, A. Muszyński, L. S. Forsberg, and R. W. Carlson for *S. typhimurium* LPS. Most authors were employees of Genentech, Inc.

Author Contributions N.K., I.B.S., B.L.L., K.O., T.C., B.H., P.S.L., Q.T.P., J.R.L., H.L., J.W., S.K., J.Z., W.P.L., S.J.S., L.X.M., L.F., Y.Z. and E.M.B. designed and performed experiments. K.A. and S.W. generated *Gsdmd*^{-/-} mice. S.W. and M.R.-G. generated Casp1^{-/-} mice. N.K. and E.M.B. prepared the manuscript. N.K., G.S.S., E.M.B., C.C.G. and V.M.D. contributed to the study design and data analyses.

Author Information Reprints and permissions information is available at www.nature.com/reprints. The authors declare no competing financial interests. Readers are welcome to comment on the online version of the paper. Correspondence and requests for materials should be addressed to N.K. (kayagaki@gene.com) or V.M.D. (dixit@gene.com).

METHODS

ENU-mutagenized mouse strains. Third-generation (G3) offspring used for the phenotypic screen were from ENU-treated C57BL/6 mice as described¹⁰. 129X1/SvJ strain was used as a *Casp11* mutant¹ control. All animals were housed under specific-pathogen-free conditions at the Australian Phenomics Facility. Animal experiments were approved by the Australian National University Animal Ethics and Experimentation Committee.

Exome capture and sequencing of G1 founder. Exome-enriched, paired-end libraries were prepared from genomic DNA of first generation (G1) mice using the Agilent SureSelect XT2 Mouse All Exon kit (Agilent) following the manufacturer's instructions. Each sample was prepared with an index and then pooled in a batch of six in equimolar amounts before exome enrichment. Each 6-plex exome-enriched library was sequenced in one lane of an Illumina HiSeq2000 with version 2 chemistry as 100-bp paired-end reads. ENU variants were identified as described previously⁴¹. In brief, sequence reads were mapped to the GRCm38 assembly of the reference mouse genome using the default parameters of the Burrows-Wheeler Aligner (BWA, <http://bio-bwa.sourceforge.net>). Untrimmed reads were aligned allowing a maximum of two sequence mismatches and were discarded where they aligned to the genome more than once. Sequence variants were identified with SAMtools (<http://samtools.sourceforge.net>) and annotated using Annovar (<http://www.openbioinformatics.org>). PolyPhen2 (<http://genetics.bwh.harvard.edu/pph2>) and SIFT (<http://sift.jcvi.org/>) were used for the calculation of variant effect. Variants were filtered to prioritize novel variants not in dbSNP (or in a list of common mouse variants identified by the pipeline) and predicted to be deleterious to the protein by PolyPhen and/or SIFT. For variant validation, G1 samples were genotyped for the ENU variants identified by the exome sequencing using a competitive, allele-specific dual FRET-based assay, KASP (LGC). For genotyping of G3 offspring and IGL1351 pedigree, primers were designed based on the SNV locus-flanking sequence. Plates were read in a FLUOstar Optima (BMG Labtechnologies) plate reader.

Other mice. *Nlrp3*^{-/-}, *Asc*^{-/-}, and *Casp11*^{-/-} mice on a C57BL/6N background were described previously¹. *Il1b*^{-/-} mice generated from AB2.2 ES cells (129S7) were obtained from Taconic and backcrossed to C57BL/6J up to the N10 generation. C57BL/6-type *Casp11* genotype was confirmed by PCR as described¹. *Gsdmd*^{-/-} mice were obtained by cytoplasmic injection of C57BL/6N zygotes with 25 ng μ l⁻¹ wild-type Cas9 mRNA (Life Technologies) and 13 ng μ l⁻¹ *in vitro*-transcribed single-guide RNA (gRNA) prepared by MEGAshortscript T7 Kit (Life Technologies). Tail DNA from resulting offspring was analysed by PCR and sequencing. Target sequences of gRNA are 5'-GAGAAGGGAAAATTCTGG (G9) and 5'-AGGG

CAGAGTGATGTTGTC (G2). Allele sequences of *Gsdmd*^{-/-} mice used are provided in Extended Data Fig. 8. *Casp1*^{-/-} mice (Extended Data Fig. 7d) lacking exons 1 and 2 were generated at Genentech from gene-targeted C57BL/6N C2 ES cells. *Casp1*^{-/-} mice were genotyped with PCR primers (5'-CCTGAATCTTAGACCAAGTTGAG; 5'-AGGCAGAAGGAATAGGAATAGT and 5'-CCAGGTATCTCAATCACATGGT) yielding a 167-bp wild-type DNA fragment and a 287-bp mutant DNA fragment. The Genentech Institutional Animal Care and Use Committee approved all animal studies.

Reagents and antibodies. Ultra-pure LPS (*E. coli* O111:B4), Pam3CSK4, poly(I:C) LMW, R837 (Imiquimod), dsDNA (poly(dA:dT)), ultra-pure flagellin (*P. aeruginosa*), MSU, and CPPD were from Invivogen. Other reagents were synthetic monophosphoryl lipid A (Enzo Life Sciences), TcdB, cholera toxin B (Ctb; List Biological Laboratories), LLO toxin (ReagentProteins), HLLome (Chem Impex International), IFN- α , (PBL Assay Science), IFN- γ (eBioscience), and ATP (Sigma). LPS from *S. typhimurium* was described previously^{42,43}. Antibodies used include: mouse caspase-1 (clone 4B4, Genentech), human caspase-1 (Bally-1, AdipoGen), caspase-4 (4B9, Enzo Life Sciences), caspase-5 (4429, Cell Signaling Technology), caspase-11 (clone 17D9, Novus Biologicals), Gsdmd (G7422 anti-Gsdmd aa 126-138, Sigma), IL-1 β (GTX74034, GeneTex), NLRP3 (clone Cryo-2, AdipoGen), and Flag epitope (M2, Sigma).

Macrophage cultures. Bone marrow cells were differentiated in DMEM supplemented with 10% endotoxin-free fetal bovine serum (Omega Scientific) and 20% M-CSF-conditioned medium for 5–6 days. Adherent BMDMs or thioglycollate-elicited peritoneal macrophages were cultured overnight in 96-well plates at 1×10^6 cells per ml before being primed for 5–6 h with 1μ g ml⁻¹ Pam3CSK4 in OPTI-MEM (Life Technologies). Primed cells were transfected with 2μ g ml⁻¹ LPS or 5μ g ml⁻¹ lipid A by using 0.25% v/v FuGENE HD (Promega) or 20μ g ml⁻¹ Ctb, or electroporated with 2μ g ml⁻¹ LPS by using the 4D-Nucleofector system (Lonza) as described previously⁷. Unless specified, FuGENE HD was used for the LPS transfection. The other conditions for inflammasome activations were 5 mM ATP, 100 ng ml⁻¹ TcdB, 2μ g ml⁻¹ dsDNA plus 0.1% v/v Lipofectamine 2000 (Life Technologies), 0.5 μ g ml⁻¹ flagellin plus 0.25% v/v FuGENE HD, 1 mg ml⁻¹ MSU, 500 μ g ml⁻¹ CPPD, and 1 mM HLLome. Infections with *P. aeruginosa* (ATCC 27853; multiplicity of infection (MOI) 25), *E. coli* (ATCC 11775, MOI

30), *C. rodentium* (ATCC 51116, MOI 20), or *S. flexneri* (ATCC 9199, MOI 20) were for 1.5 h and then cultures were supplemented with 100μ g ml⁻¹ Gentamycin (Life Technologies). For stimulation with TLR agonists or interferons, BMDMs were cultured with 1μ g ml⁻¹ Pam3CSK4, 5μ g ml⁻¹ polyI:C, 5μ g ml⁻¹ LPS, 2μ g ml⁻¹ R848, 75 ng ml⁻¹ IFN- α , or 500 ng ml⁻¹ IFN- γ for the indicated periods. ELISAs were used to measure IL-1 β (Meso Scale Discovery) in culture supernatants. A CytoTox 96 Non-Radioactive Cytotoxicity assay (Promega) measured cell death. For measuring RANTES, Luminex assay (Cocktail (Roche)) was used. Each figure legend shows the number of samples per experiment and number of experiments that were analysed independently. For immunoblotting, cells were lysed with RIPA buffer (50 mM Tris-HCl pH 7.4, 150 mM NaCl, 1 mM EDTA, 1 \times Complete Protease Inhibitor (Roche), 1% Triton X-100, 0.1% SDS). For cleavage studies (Gsdmd p30, caspase-1 p20, and IL-1 β p17), pooled culture supernatants and cell extracts were precipitated with 7.2% trichloroacetic acid plus 0.15% sodium deoxycholate.

Recombinant proteins. DNA encoding Flag-tagged caspase-11 (residues 2–373) and His6-MBP-tagged murine Gsdmd (residues 2–487) were generated by gene synthesis, and subcloned into a modified version of pAcgp67 (BD Biosciences). Transfer vectors were co-transfected with BestBac linearized viral DNA (Expression Systems) into Sf9 cells (Life Technologies) using Transit-IT-Insect transfection reagent (Mirus Bio) to produce recombinant baculovirus. The virus was amplified twice to prepare the stock used for protein expression. Protein was expressed in *Tni* pro cells (Expression Systems). A 22 l Wave bioreactor was inoculated with *Tni* pro cells at 1×10^6 cells per ml in serum-free ESF921 (Expression Systems). At 48 h post infection, the *Tni* cells were harvested and frozen at -80°C . For the purification of Gsdmd, the baculovirus cell pellets were thawed and lysed in lysis buffer (50 mM Tris-HCl pH 8.0, 150 mM NaCl, 20 mM imidazole, 1 mM TCEP plus Protease Inhibitor Cocktail (Roche)). The cell lysate was loaded onto a 3 ml NiNTA column (QIAGEN) pre-equilibrated with buffer A (20 mM Tris pH 8.0, 300 mM NaCl, 20 mM imidazole, 0.5 mM TCEP). The column was washed with 20 column volumes buffer A, then eluted with 5 column volumes of buffer B (20 mM Tris-HCl pH 8.0, 300 mM NaCl, 250 mM imidazole, 0.5 mM TCEP). The elutant was then loaded onto a 5 ml MBP column (GE Healthcare Life Sciences) pre-equilibrated with buffer C (20 mM Tris-HCl pH 7.5, 150 mM NaCl, 10% glycerol, 0.5 mM TCEP). The MBP column was washed with 15 column volumes of buffer C. Gsdmd protein was eluted with buffer C containing 10 mM maltose. To cleave off His-MBP tag, purified His6-MBP-tagged Gsdmd was digested with TEV (Sigma). Un-cleaved Gsdmd and TEV enzyme were removed by passing through a 3 ml NiNTA column. For the purification of caspase-11, the baculovirus cell pellets were thawed and lysed in lysis buffer (50 mM Tris-HCl pH 7.5, 150 mM NaCl, 0.5 mM TCEP plus protease inhibitor cocktail) for 1 h. The cell lysate was loaded onto a 4 ml Flag column (Sigma) pre-equilibrated with buffer D (50 mM Tris-HCl pH 7.5, 150 mM NaCl, 10% glycerol, 0.5 mM TCEP). The column was washed with 5 column volumes of buffer C, then 20 column volumes of buffer E (buffer D plus 0.1% TritonX-114) followed with 15 column volumes of Buffer D. Caspase-11 was eluted with buffer F (buffer D plus 0.2 mg ml⁻¹ 3 \times Flag peptide (Sigma)). The purified recombinant caspase-11 was then concentrated and further purified by a HiLoad 16/60 Superdex 200 column with buffer G (20 mM Tris-HCl pH 7.5, 150 mM NaCl, 10% glycerol). Purified recombinant caspase-11 and Gsdmd were characterized by SDS-PAGE and mass spectrometry, and stored at -20°C .

Recombinant Gsdmd processing assay. Recombinant Gsdmd (4 μ M) was incubated in the presence or absence of 2 μ M recombinant caspase-11 at 37°C for 30 min in standard caspase reaction buffer (20 mM PIPES pH 7.2, 10% sucrose, 100 mM NaCl, 0.1% CHAPS, 1 mM EDTA, 10 mM DTT). Samples were then subjected to SDS-page followed by Coomassie blue staining (Expediton). For Edman degradation analysis, samples were blotted onto a PVDF after SDS-page electrophoresis, and the band corresponding to the Gsdmd protein fragment was subjected to N-terminal sequencing using traditional Edman chemistries⁴⁴ on a 494HT Procise sequencer (Applied Biosystems) with fast cycles⁴⁵.

Plasmids and transient expression. cDNAs encoding Gsdmd (human and mouse), human caspase-4, and caspase-5 were artificially synthesized with a Flag epitope and subcloned into pcDNA3.1/Zeo(+) (Life Technologies) for transient expression in HEK293T cells, or into pLenti6.3/V5-DEST (Life Technologies) for lentivirus production. Human codon-optimized Cas9 was synthesized and subcloned into pLenti7.3 (Life Technologies). Mutagenesis of cDNAs was performed with a QuikChange site-directed mutagenesis kit (Agilent Technologies). For transient expression, HEK293T cells (ATCC) were cultured overnight in 96-well plates at 1.2×10^5 cells per ml, then transfected with 2–10 ng of plasmids by using 0.16 μ l Lipofectamine 2000. At 24 h after transfection, cytotoxicity against HEK293T cells was measured by CellTiter-Glo (Promega). For human GSDMD processing, HEK293T cells that stably express human GSDMD were selected using 1 mg ml⁻¹ Zeocin (Invivogen) after transfection with human GSDMD plasmid. The stable

transfectant cells were transiently transfected with 20 ng of human caspase-4 or -5 plasmids as described above. At 24 h after transfection, cells were lysed with RIPA buffer for immunoblotting. HEK293T cell lines used were regularly tested for mycoplasma. All cell lines used were authenticated by short tandem repeat (STR) profiling, single nucleotide polymorphism (SNP) fingerprinting, and mycoplasma testing.

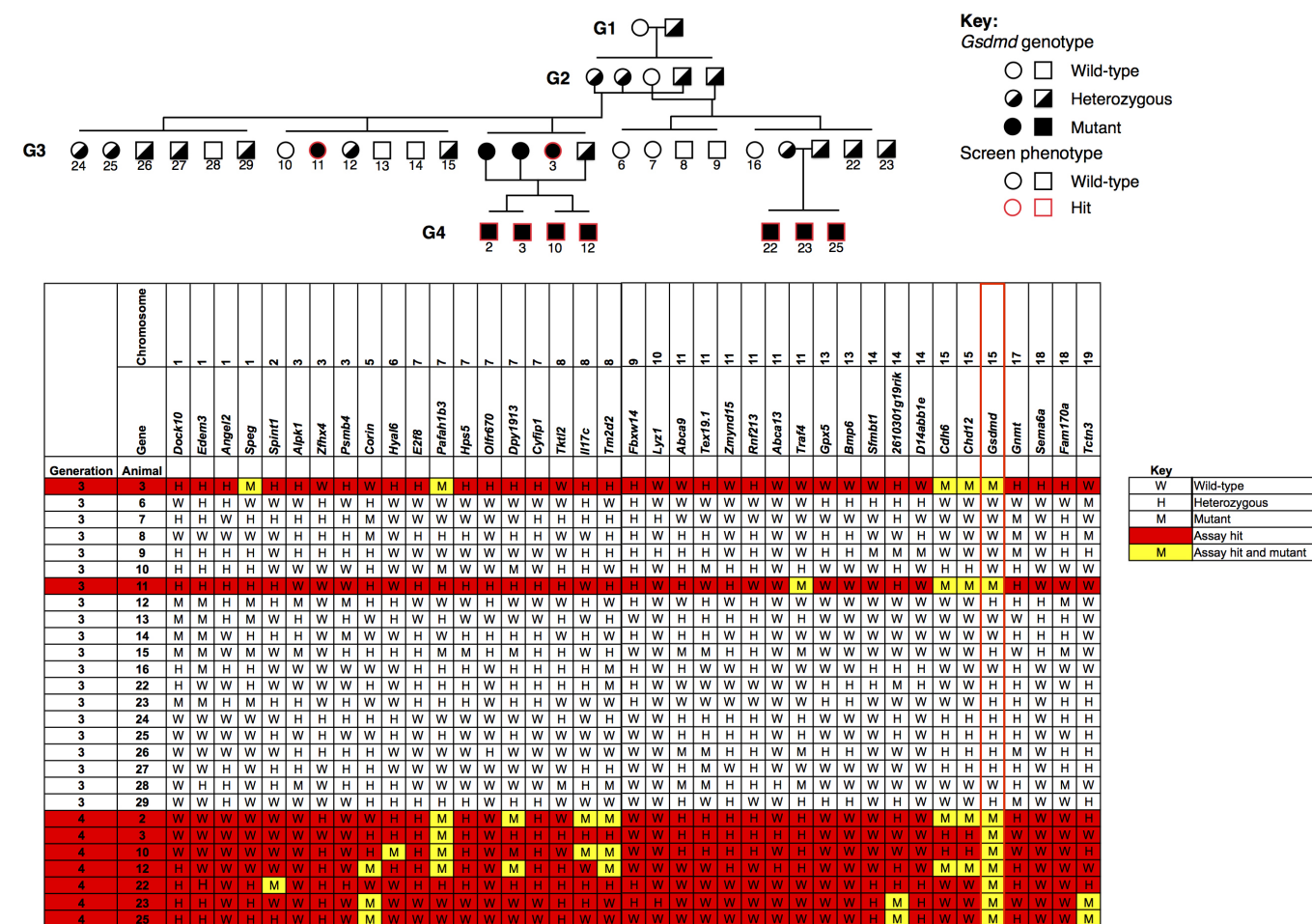
Knockout cell lines. Human EA.hy926 (ATCC) endothelial cells and human THP-1 (ATCC) monocytes were lentivirally transduced with Cas9 and single-cell cloned. gRNAs were transduced into Cas9⁺ cloned lines by lentiviral delivery with pLKO.1 vector (Sigma) followed by selection of gRNA-expressing cells by Puromycin (Life Technologies). At 11–14 days post-selection, cells were harvested for experiments. The target sequences of gRNA used are 5'-GTTGGCTTCCTGGGCTGCTA for human CD81 (control), 5'-GCATGCGAGAATCTCACGC for luciferase (control), 5'-GGTGTGTTTGGATAACTTGG for *CASP4* knockout, 5'-GTAGTCCGGA GAGTGGTCC for human *GSDMD* knockout (gRNA1), and 5'-AACCACCAG GCAGTAGGGC for human *GSDMD* knockout (gRNA2). EA.hy926 cells were transfected with 10 µg ml⁻¹ LPS by 0.5% v/v Lipofectamine 2000 or treated with 100 ng ml⁻¹ APO2L (R&D systems). At 24 h after stimulation, cytotoxicity against EA.hy926 was measured by CellTiter-Glo. THP-1 cells were primed with 0.5 µg ml⁻¹ Pam3CSK4 for 4 h, then plated in 96-well plates at 1 × 10⁶ cells per ml with OPTI-MEM containing 0.5 µg ml⁻¹ Pam3CSK4, followed by transfection of 2 µg ml⁻¹ dsDNA with 0.125% v/v Lipofectamine 2000. For LPS electroporation into Pam3CSK4-primed THP-1 cells, the Neon transfection system (Life Technologies) was used with 1 × 10⁶ cells plus LPS 0.1 µg per chamber condition. All the cell lines used were regularly tested for mycoplasma. All cell lines used were authenticated by STR profiling, SNP fingerprinting, and mycoplasma testing.

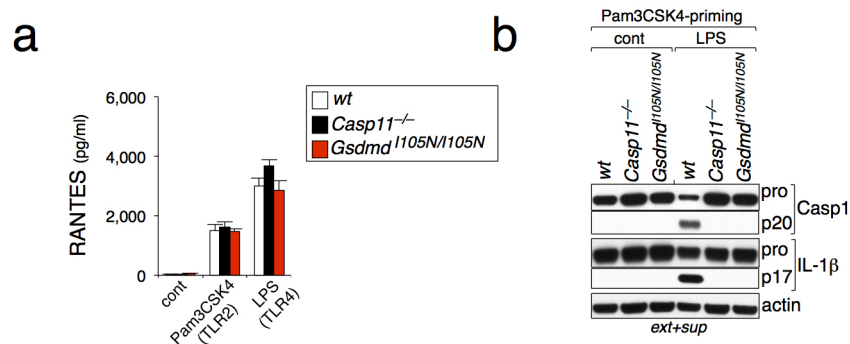
Gsdmd reconstitution. Macrophage progenitor cells from *Gsdmd*^{-/-} mice (Extended Data Fig. 8) were immortalized by ER-Hoxb8 as described previously^{46,47}. The immortalized macrophage progenitor cells were lentivirally transduced with cDNA encoding either wild-type or D276A mouse *Gsdmd* using pLenti6.3/V5-DEST vector. Cells were selected in 6.25 µg ml⁻¹ Blasticidin (Invitrogen) and

differentiated in M-CSF-containing conditioned media⁴⁸. Stimulation of ER-Hoxb8-immortalized macrophages was performed as described above. All Hoxb cell lines used were regularly tested for mycoplasma.

Endotoxic shock model. Female mice aged 8–10 weeks were injected intraperitoneally with 54 mg kg⁻¹ LPS (*E. coli* O111:B4, Sigma) and monitored eight times daily for a total of 6 days. *Gsdmd*^{-/-} mice used (*Gsdmd*^{-/-} 6–13) are described in Extended Data Fig. 8. Statistical analysis was performed with log-rank (Mantel–Cox) tests using Prism, and *P* values were adjusted to account for multiple comparisons using Bonferroni's correction. Sample sizes were chosen by standard methods to ensure adequate power and no mice were excluded from the analysis. No randomization or blinding was used for the animal studies. No statistical method was used to estimate sample size. The Genentech Institutional Animal Care and Use Committee approved all animal studies.

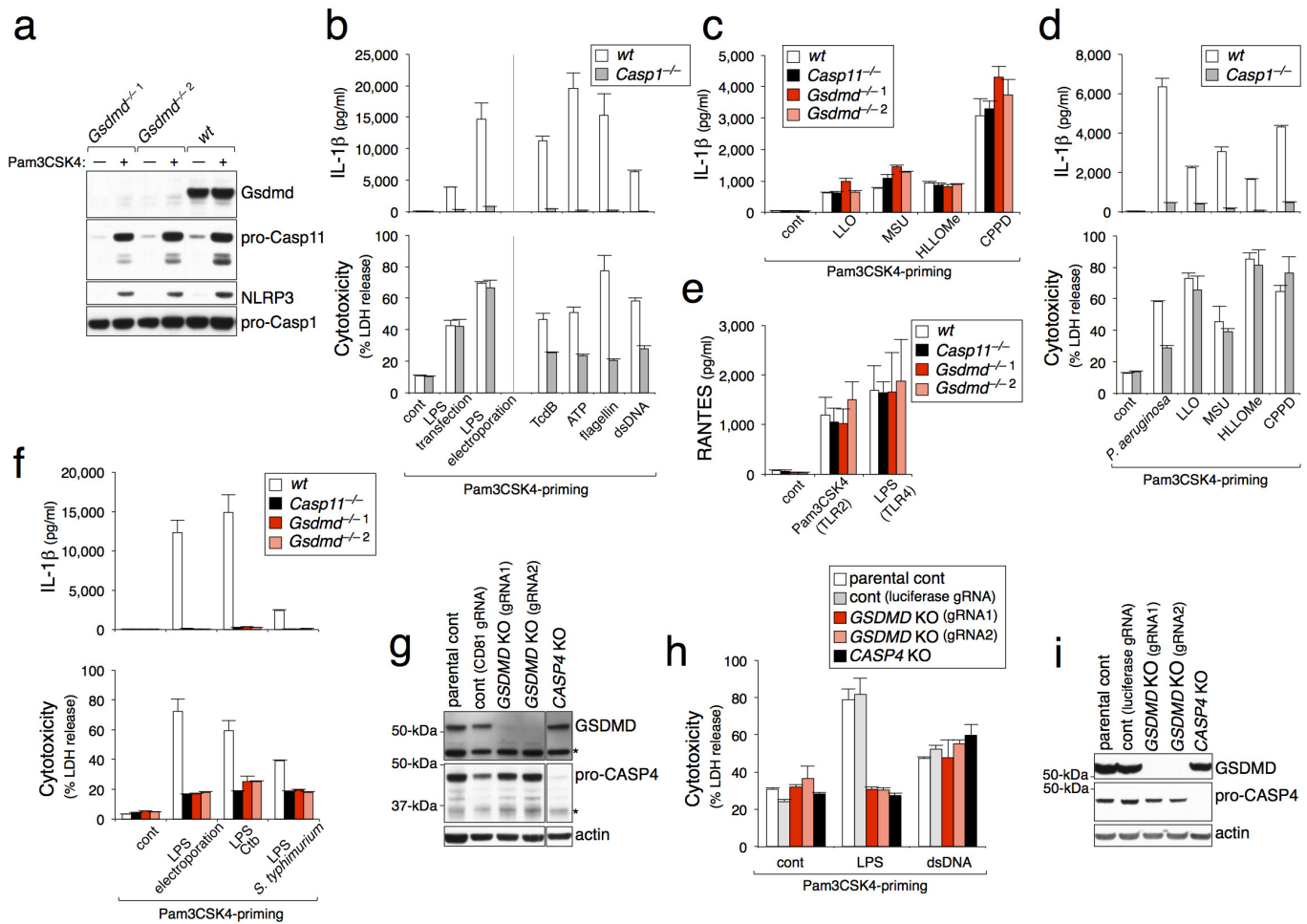
41. Andrews, T. D. *et al.* Massively parallel sequencing of the mouse exome to accurately identify rare, induced mutations: an immediate source for thousands of new mouse models. *Open Biol.* **2**, 120061 (2012).
42. Carlson, R. W., Forsberg, L. S. & Kannenberg, E. L. Lipopolysaccharides in Rhizobium-legume symbioses. *Subcell. Biochem.* **53**, 339–386 (2010).
43. Tamayo, R. *et al.* Identification of *cptA*, a *PmrA*-regulated locus required for phosphoethanolamine modification of the *Salmonella enterica* serovar typhimurium lipopolysaccharide core. *J. Bacteriol.* **187**, 3391–3399 (2005).
44. Edman, P. A method for the determination of amino acid sequence in peptides. *Arch. Biochem.* **22**, 475 (1949).
45. Henzel, W. J., Tropea, J. & Dupont, D. Protein identification using 20-minute Edman cycles and sequence mixture analysis. *Anal. Biochem.* **267**, 148–160 (1999).
46. Wang, G. G. *et al.* Quantitative production of macrophages or neutrophils *ex vivo* using conditional Hoxb8. *Nature Methods* **3**, 287–293 (2006).
47. Qu, Y. *et al.* Phosphorylation of NLRC4 is critical for inflammasome activation. *Nature* **490**, 539–542 (2012).
48. Rosas, M. *et al.* Hoxb8 conditionally immortalised macrophage lines model inflammatory monocytic cells with important similarity to dendritic cells. *Eur. J. Immunol.* **41**, 356–365 (2011).





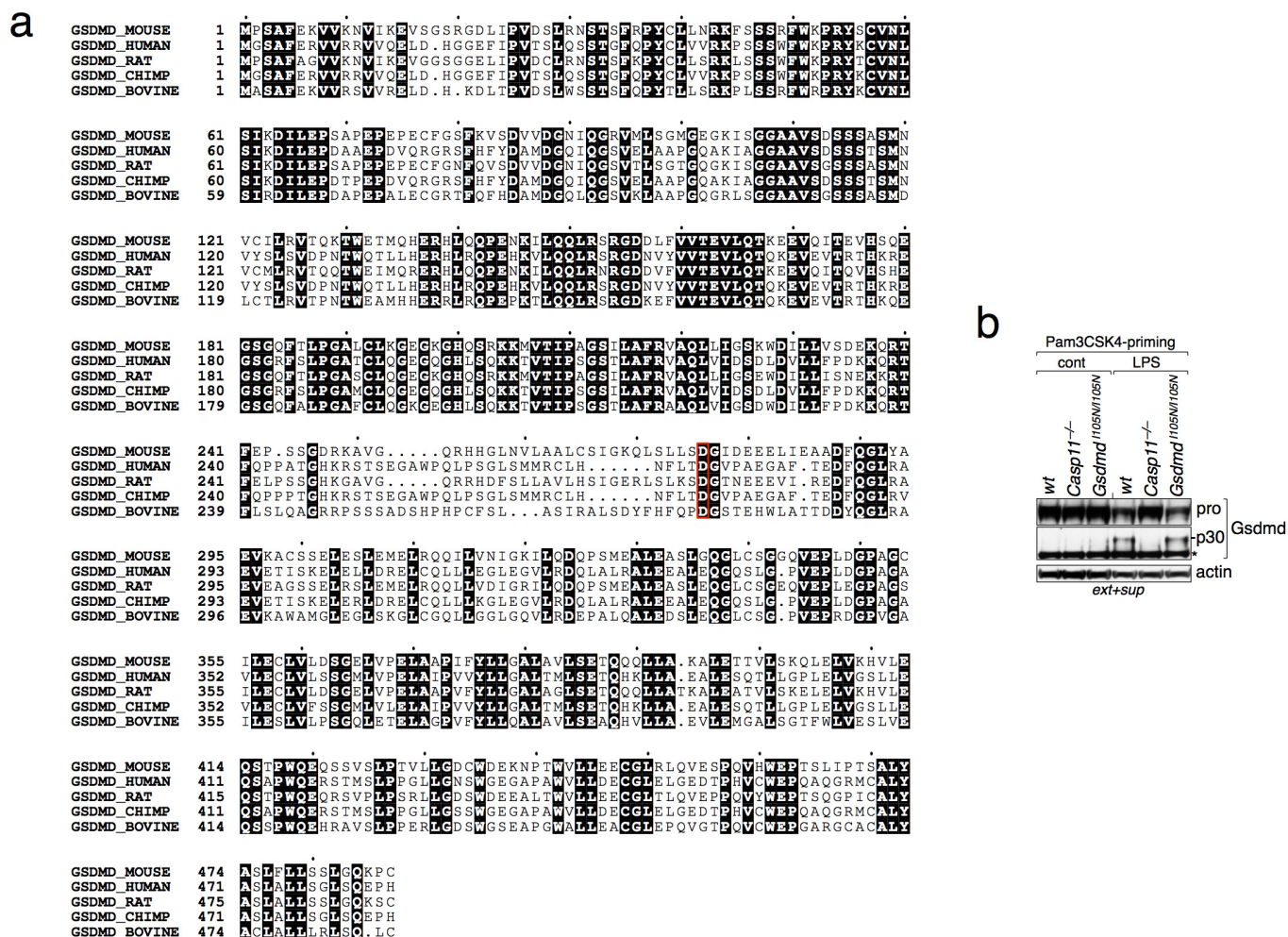
Extended Data Figure 2 | *Gsdmd*^{I105N/I105N} BMDMs respond normally to TLR agonists. **a**, RANTES production from BMDMs cultured for 16 h with medium alone (cont) or the TLR stimulants indicated. **b**, Western blots of

BMDM extracts and supernatants at 6 h after LPS electroporation. Graph shows the mean \pm s.d. of triplicate wells and represents three independent experiments. For source gel, see Supplementary Fig. 2.



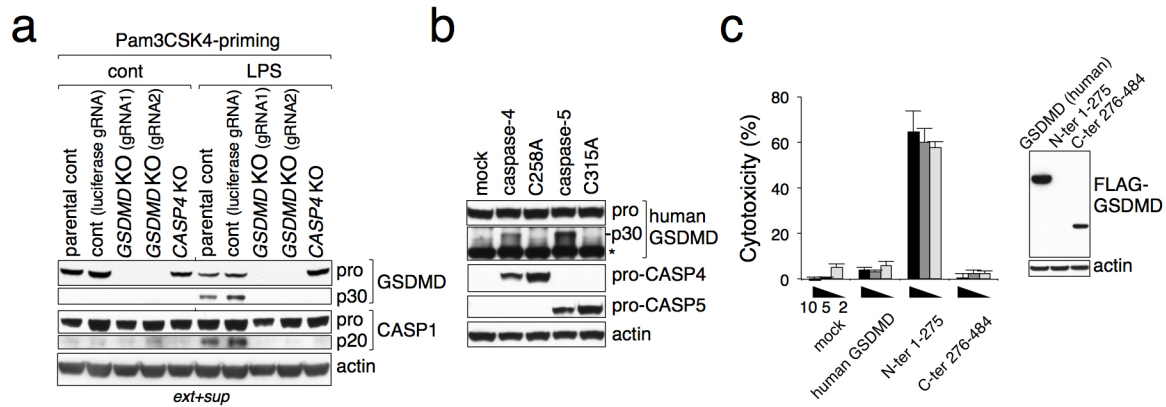
Extended Data Figure 3 | Non-canonical inflammasome signalling requires *Gsdmd*. **a**, Western blots of BMDMs cultured with or without Pam3CSK4 for 6 h. *Gsdmd*^{-/-1} and *Gsdmd*^{-/-2} are independent knockout strains. **b-d**, IL-1β and LDH released from BMDMs after 16 h. *P. aeruginosa* infection was analysed at 4 h. **e**, RANTES production from BMDMs after 16 h. **f**, IL-1β and LDH released from BMDMs at 16 h after LPS electroporation, LPS plus cholera toxin B (Ctb) complex, or *S. typhimurium* LPS transfection.

g, i, Western blots of EA.hy926 (**g**) or THP-1 cells (**i**). **h**, LDH released from control (parental or luciferase gRNA), *GSDMD* knockout (KO), or *CASP4* knockout THP-1 cells at 16 h after LPS electroporation or dsDNA transfection. Graphs show mean ± s.d. of triplicate wells and represent three independent experiments. For source gels of **a**, **g** and **i**, see Supplementary Information Fig. 2.



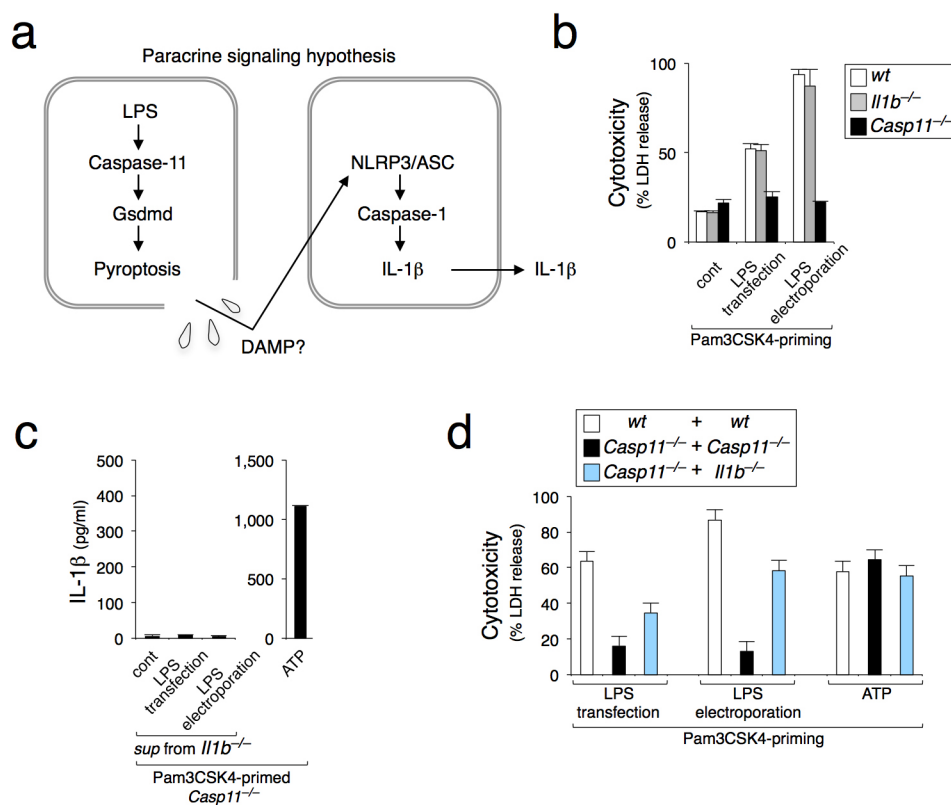
Extended Data Figure 4 | Gsdmd cleavage site. **a**, Alignment of Gsdmd amino acid sequences. The conserved Gsdmd cleavage site (D276 in mouse) is boxed in red. **b**, Immunoblots of BMDM extracts and supernatants at 16 h after

LPS/Ctb treatment. A non-specific band is indicated with an asterisk. Cont, Ctb alone. For source gel, see Supplementary Fig. 3.



Extended Data Figure 5 | Human GSDMD processing. **a**, Western blots of THP-1 extracts and supernatants at 3 h after LPS electroporation. **b**, Western blots of human GSDMD/HEK293T stable transfectants at 24 h after transient transfection of the indicated plasmids. A non-specific band is indicated with an asterisk. **c**, Cytotoxicity of the human proteins indicated at 24 h after transient transfection of HEK293T cells. Numbers indicate

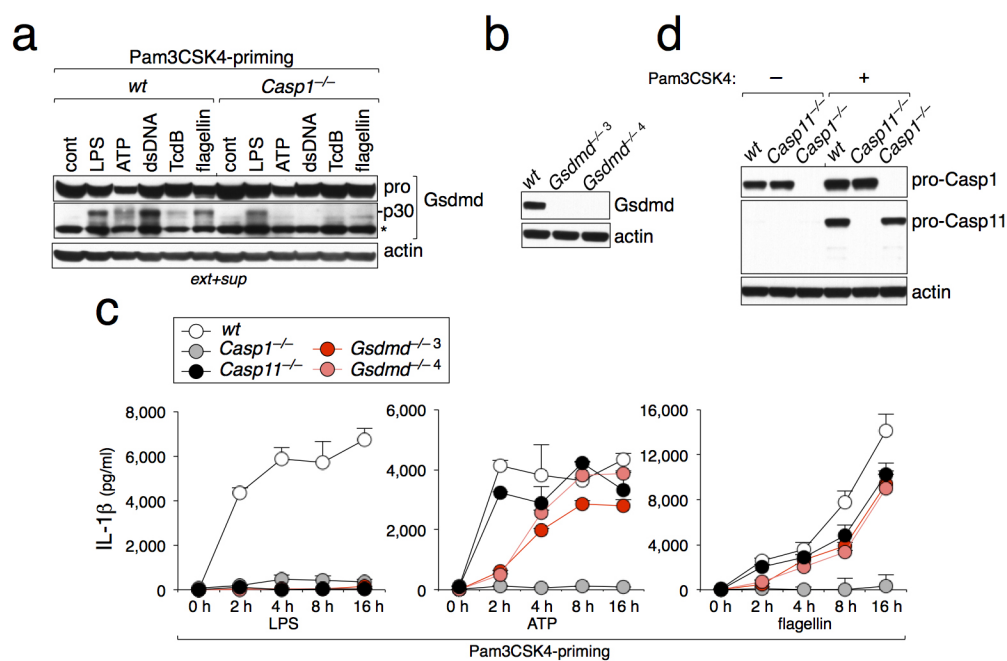
nanograms of plasmid transfected. Western blots (right) indicate protein expression. Expression of the N-terminal fragment (1–275) was below detection levels, presumably due to its potent toxicity. Graph shows mean \pm s.d. of triplicate wells and represents three independent experiments. For source gels of **a**, **b** and **c**, see Supplementary Fig. 3.



Extended Data Figure 6 | BMDMs stimulated with cytoplasmic LPS do not release NLRP3-stimulating damage-associated molecular pattern activity.

a, Paracrine signalling hypothesis. DAMP, damage-associated molecular pattern. **b**, LDH released from BMDMs at 16 h after LPS transfection or electroporation. **c**, IL-1 β released from *Casp11*^{-/-} BMDMs at 16 h after

stimulation with ATP or incubation with *Il1b*^{-/-} BMDM culture supernatants derived in **b**. **d**, LDH released from 1:1 mixed cultures of the indicated BMDMs at 16 h after stimulation. Graphs show mean \pm s.d. of triplicate wells and represent three independent experiments.



Extended Data Figure 7 | Canonical inflammasome stimuli induce caspase-1-dependent processing of Gsdmd. **a**, Western blots of BMDM extracts and supernatants at 8 h after stimulation. Cont, medium alone. LPS, LPS + Ctb. Asterisk indicates a non-specific band. **b**, Western blots of *Gsdmd*^{-/-} BMDMs. *Gsdmd*^{-/-3} and *Gsdmd*^{-/-4} are independent knockout strains (Extended Data

Fig. 8). **c**, IL-1β released from BMDMs. LPS, LPS electroporation. Graphs show mean ± s.d. of triplicate wells and represent three independent experiments. **d**, Immunoblots of *Casp1*^{-/-} BMDMs stimulated with Pam3CSK4 for 5 h. For source gels of **a**, **b** and **d**, see Supplementary Fig. 3.

Wt gRNA G9 target region

AGTGATGTTGTCAGGCATGGG**GAGAAGGGAAAAATTTCTGGT**GGGGCTGCAGTGTCTGAC
 .ValMetSerLeuGlyMetGlyGluGlyLysIleSerGlyGlyAlaAlaValSerAsp..

***Gsdmd*^{-/-1} (1bpTdel/1bpGins)**

allele1: AGTGATGTTGTCAGGCATGGG**GAGAAGGGAAAAATTTCTGGT**GGGGCTGCAGTGTCTGAC
 allele2: AGTGATGTTGTCAGGCATGGG**GAGAAGGGAAAAATTTCTGGT**GGGGCTGCAGTGTCTGAC

***Gsdmd*^{-/-2} (1bpTdel/1632bpdel)**

allele1: AGTGATGTTGTCAGGCATGGG**GAGAAGGGAAAAATTTCTGGT**GGGGCTGCAGTGTCTGAC
 allele2: -----

***Gsdmd*^{-/-3} (1bpTins/1bpTins)**

allele1: AGTGATGTTGTCAGGCATGGG**GAGAAGGGAAAAATTTCTGGT**GGGGCTGCAGTGTCTGAC
 allele2: AGTGATGTTGTCAGGCATGGG**GAGAAGGGAAAAATTTCTGGT**GGGGCTGCAGTGTCTGAC

***Gsdmd*^{-/-5} (90bpdel+3bpins/10bpdel+5bpins)**

allele1: AGTGATGTTGTCAGGCATGGG**GAGAAGGGAAAAATTTCT**-----
 allele2: AGTGATGTTGTCAGGCATGGG**GAGAAGGG**-----**TGACC**GTGGGGCTGCAGTGTCTGAC

Wt gRNA G2 target region

CGATGGGAACATTCAGGG**CAGAGTGATGTTGTC**AGGCATGGGAGAAGGGAAAAATTTTC
 .AspGlyAsnIleGlnGlyArgValMetLeuSerGlyMetGlyGluGlyLysIle...

***Gsdmd*^{-/-4,6-9} (2bpATins/19bpdel)**

allele1: CGATGGGAACATTCAGGG**CAGAGTGATGTTATGTC**AGGCATGGGAGAAGGGAAAAATTTTC
 allele2: CGATGGGAACATTCAGG-----CATGGGAGAAGGGAAAAATTTTC

***Gsdmd*^{-/-10} (2bpATins/2bpATins)**

allele1: CGATGGGAACATTCAGGG**CAGAGTGATGTTATGTC**AGGCATGGGAGAAGGGAAAAATTTTC
 allele2: CGATGGGAACATTCAGGG**CAGAGTGATGTTATGTC**AGGCATGGGAGAAGGGAAAAATTTTC

***Gsdmd*^{-/-13} (19bpdel/19bpdel)**

allele1: CGATGGGAACATTCAGG-----CATGGGAGAAGGGAAAAATTTTC
 allele2: CGATGGGAACATTCAGG-----CATGGGAGAAGGGAAAAATTTTC

gRNA G2/G9***Gsdmd*^{-/-11} (G2:1bpTins/G9:5bpdel)**

allele1: CGATGGGAACATTCAGGG**CAGAGTGATGTTGTC**AGGCATGGGAGAAGGGAAAAATTTTC
 allele2: AGTGATGTTGTCAGGCATGGG**GAGAAGGGAAAA**-----**GGT**GGGGCTGCAGTGTCTGAC

***Gsdmd*^{-/-12} (G2:203bpdel/G9:4bpdel)**

allele1: -----
 allele2: AGTGATGTTGTCAGGCATGGG**GAGAAGGGAAAAAT**-----**GGT**GGGGCTGCAGTGTCTGAC

Extended Data Figure 8 | *Gsdmd*^{-/-} alleles. *Gsdmd*^{-/-} animals used in this study were compound or homozygous F1 and F2 knockouts generated from mosaic F0 founder and F1 crosses, respectively. gRNA target sequences are highlighted in bold. Deleted bases are indicated by red hyphens. Inserted nucleic acids are highlighted in red.

Extended Data Table 1 | Bioinformatic analysis of ENU-induced SNVs present in IGL1351 pedigree

Chromosome	Coordinate (Assembly version: GRCm38)	Amino Acid Change	Splice Position	Polyphen Score	Polyphen Prediction	SIFT Score	SIFT Prediction	MGI accession Id	Gene Name	Ref Base	Var Base	Amino acid position	Codon
1	75411276		10					MGI:109282	Spag	T	A		
1	80593159	K->N		0.90	Possibly damaging	0.02	deleterious	MGI:2146320	Dock10	T	G	339	TTT
1	151792385	V->A		0.79	Possibly damaging	0.00	deleterious	MGI:1914217	Edem3	T	C	305	GTC
1	190933113	N->K		0.00	Benign	0.28	tolerated	MGI:1196310	Angpt2	C	A	102	AAC
2	119246455	D->G		1.00	Probably damaging	0.01	deleterious	MGI:1338033	Spint1	A	G	340	GAT
3	5401136	Y->C		1.00	Probably damaging	0.02	deleterious	MGI:2137668	Zfhx4	A	G	2118	TAT
3	94886227	Disrupted splicing	6					MGI:1098257	Pamb4	A	T		
3	127672362	Q->R		0.96	Probably damaging	0.00	deleterious	MGI:1918731	Atpk1	T	C	1165	TTG
5	72338951	C->S		1.00	Probably damaging	0.00	deleterious	MGI:1349451	Corin	A	T	673	ACA
6	24734179	F->S		1.00	Probably damaging	0.00	deleterious	MGI:1921659	Hyal6	T	C	37	TTC
7	25295145	R->C		0.98	Probably damaging	0.00	deleterious	MGI:108414	Pafah1b3	G	A	215	ACG
7	35727415	Disrupted splicing	4					MGI:2443952	Dpy19l3	A	G		
7	46761432	M->I		1.00	Probably damaging	0.14	tolerated	MGI:2183207	Hps5	C	T	1113	CAT
7	48867151	T->A		0.12	Benign	0.23	tolerated	MGI:1922038	E2f8	T	C	827	GGT
7	55898243	Y->Stop			N/A			MGI:1338801	Cyfp1	C	A	560	TAC
7	104960739	Disrupted splicing	9					MGI:3030504	Olf670	T	A		
8	25020557	Disrupted splicing	3					MGI:1916992	Tm2d2	A	G		
8	66512896	I->V		0.00	Benign	0.07	tolerated	MGI:1921669	Tkx2	A	G	369	ATC
8	122422123	T->I		0.14	Benign	0.04	deleterious	MGI:2446486, MGI:5141853	Il17c.gm20388	C	T	2	ACC
9	109274572	D->G		0.02	Benign	0.41	tolerated	MGI:1354703	Fbxw14	T	C	347	GTC
10	117291188	C->R		1.00	Probably damaging	0.00	deleterious	MGI:96902	Lyz1	A	G	45	ACA
11	9267565	S->P		1.00	Probably damaging	0.01	deleterious	MGI:2388707	Abca13	T	C	336	TCA
11	70463590	N->K		0.03	Benign	0.90	tolerated	MGI:3603821	Zmynd15	C	A	426	AAC
11	78165400	R->L		0.99	Probably damaging	0.03	deleterious	MGI:1202880	Traf4	C	A	14	CCG
11	110148903	Y->C		0.94	Probably damaging	0.02	deleterious	MGI:2386796	Abca9	T	C	428	GTA
11	119483118	V->A		0.04	Benign	0.18	tolerated	MGI:1289196	Rn213	T	C	5010	GTC
11	121147246	D->E		0.97	Probably damaging	0.11	tolerated	MGI:1920929	Tex19.1	T	A	143	GAT
13	21287499	D->G		1.00	Probably damaging	0.00	deleterious	MGI:104886	Gpx5	T	C	178	GTC
13	38469634	S->P		0.02	Benign	0.21	tolerated	MGI:88182	Bmp6	T	C	226	TCC
14	27464301	E->G		0.06	Benign	0.16	tolerated	MGI:1921694	D14abbb1e	A	G	819	GAG
14	30769820	V->A		0.00	Benign	0.22	tolerated	MGI:1859609	Sfmbt1	T	C	17	GTA
14	70145862	T->A		0.99	Probably damaging	0.25	tolerated	MGI:2444228	2610301g19rik	T	C	229	AGT
15	13034240	A->E		0.93	Possibly damaging	0.00	deleterious	MGI:107435	Ctnb1	G	T	778	TGC
15	21237903	V->M		0.99	Probably damaging	0.00	deleterious	MGI:109503	Cdh12	G	A	75	GTG
15	75864337	I->N		0.98	Probably damaging	0.00	deleterious	MGI:1916396	Gsdmd	T	A	105	ATT
17	46726680	D->G		0.01	Benign	0.01	deleterious	MGI:1202304	Gnmt	T	C	124	ATC
18	47281302	K->E		0.23	Benign	0.69	tolerated	MGI:1203727	Sema6a	T	C	520	CTT
18	50281778	W->R		0.00	Benign	0.96	tolerated	MGI:2694939	Fam170a	T	C	164	TGG
19	40607637	I->V		0.00	Benign	1.00	tolerated	MGI:1914840	Tctn3	T	C	309	GAT

Ref Base, reference base. Var Base, variant base.

Extended Data Table 2 | Adjusted *P* values of Fig. 6

Group	-Group	Adjusted p-value
<i>wt</i>	<i>Casp11^{-/-}</i>	0.0002
<i>wt</i>	<i>Gsdmd^{-/-}</i>	0.0002
<i>Casp11^{-/-}</i>	<i>Gsdmd^{-/-}</i>	0.287